

Supporting Information

The Directional Structure Transition of MnO₂ during Drying Process

Kailun Wang, Qin Cheng, Jia-qi Bai, Fang Chen, Jingshuai Chen*, Mingyuan Wu,

Song Sun, and Chang-Jie Mao

[†]School of Chemistry and Chemical Engineering, Key Laboratory of Structure and Functional Regulation of Hybrid Materials (Ministry of Education), Anhui University, Hefei, Anhui 230601, China

* Corresponding author

E-mail addresses: chen_jshuai@ahu.edu.cn

Number of Pages: 18 (S1 to S18)

Number of Figures: 11 (S1 to S14) Number of Tables: 1 (S1)

Preparation of $\text{Na}^+/\delta\text{-MnO}_2$

0.043 mol MnSO_4 was mixed in 100 mL of DI water via sonication for 15 min, after that, 100 mL of 0.05 mol NaMnO_4 was slowly added to the above solution within 5 min under vigorous magnetic stirring, followed by stirring at 80 °C for 100 minutes. After cooling down to room temperature, the precipitates were collected by centrifugation and washed several times with DI water.

After washing, equal amount of wet materials were put into three identical containers, each container was sealed with a cap with a small hole, and the drying rate of the materials in the container was adjusted by changing the size of the hole.

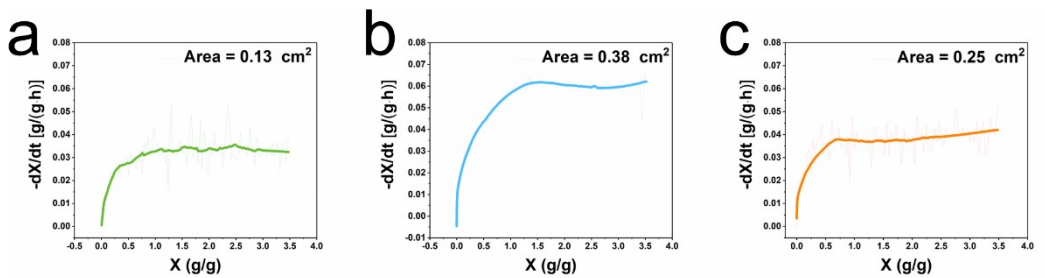


Fig. S1 The drying rate curves (a) in the case of Area = 0.13 cm^2 , (b) in the case of Area = 0.38 cm^2 , (c) in the case of Area = 0.25 cm^2 .

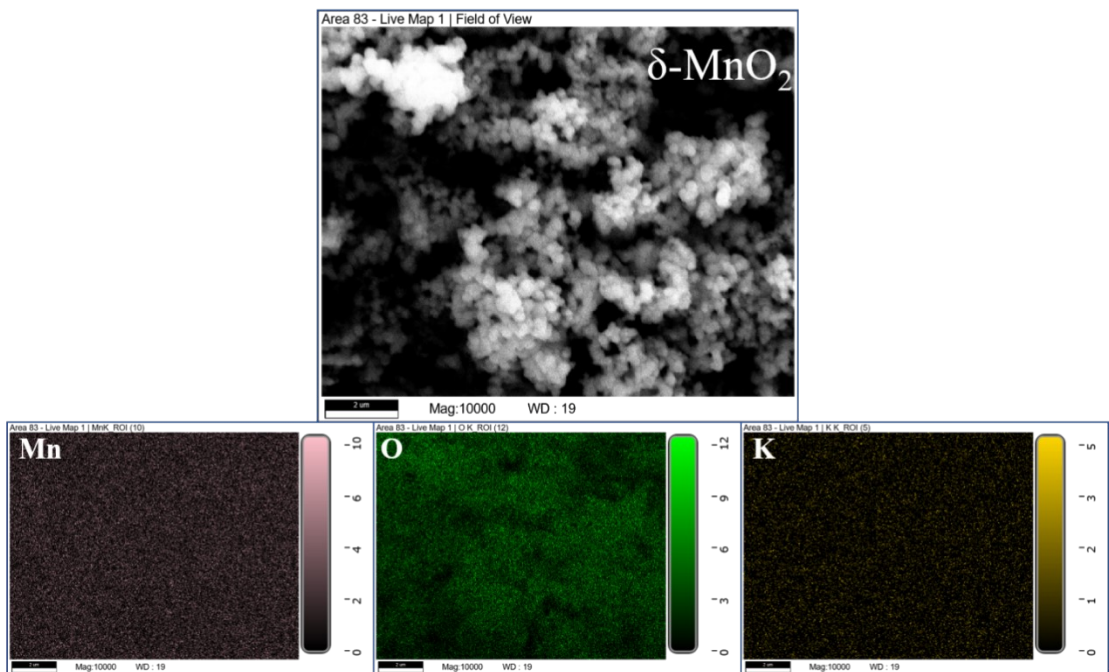


Fig. S2 EDS mapping of $\delta\text{-MnO}_2$.

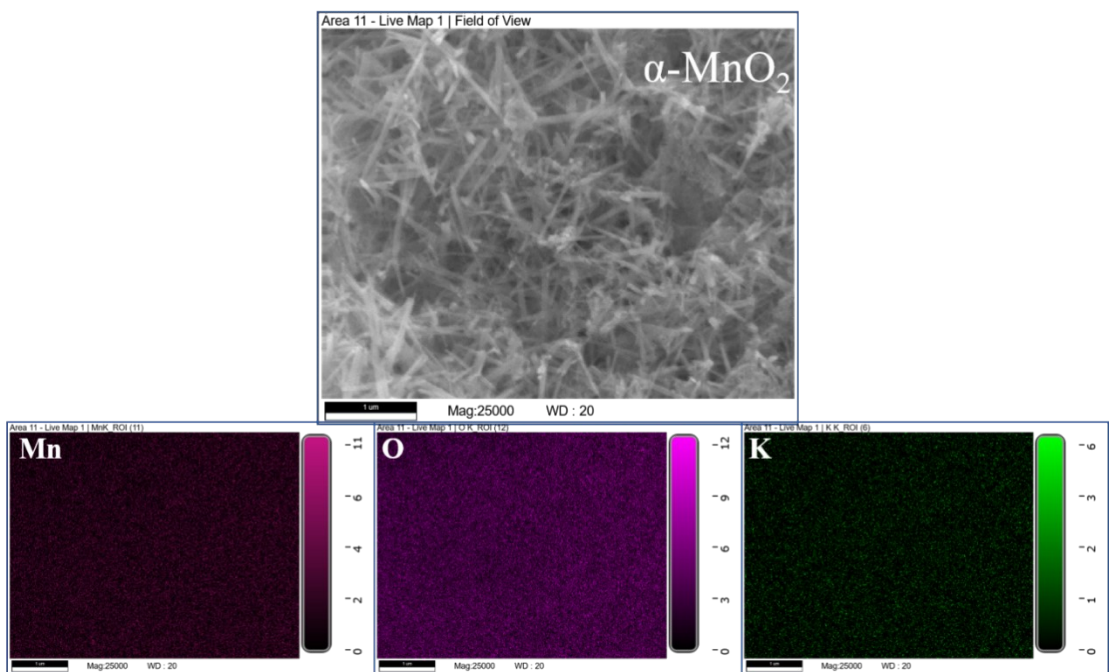


Fig. S3 EDS mapping of $\alpha\text{-MnO}_2$.

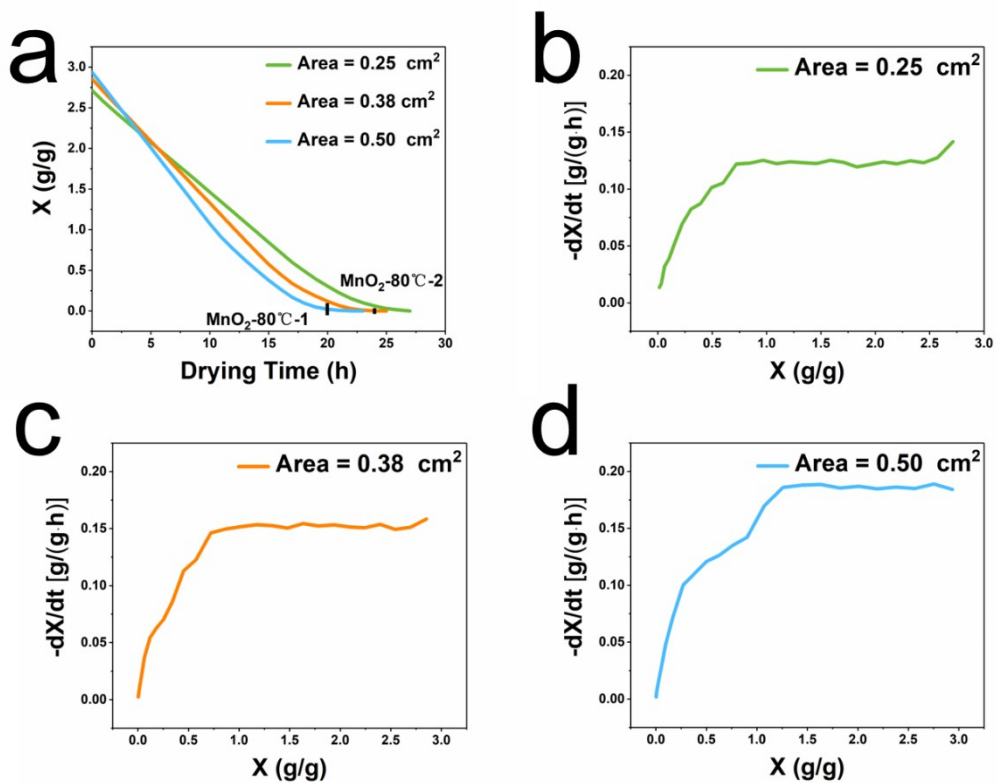


Fig. S4 The drying curves (a) in the case of Area = 0.25 cm², Area = 0.38 cm² and Area = 0.50 cm². The drying rate curves (b) in the case of Area = 0.25 cm², (c) in the case of Area = 0.38 cm², (d) in the case of Area = 0.50 cm².

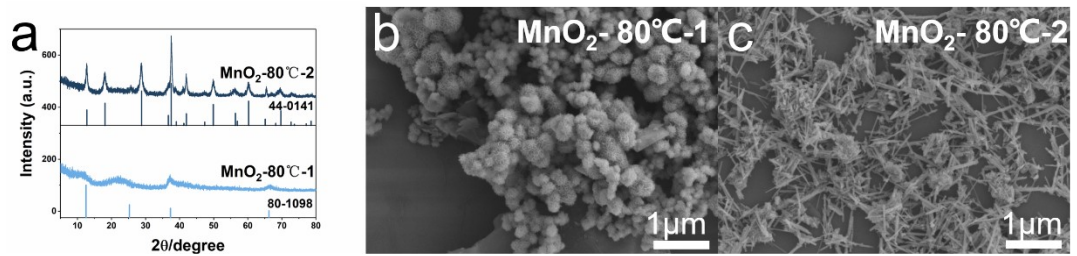


Fig. S5 XRD patterns (a) and SEM images (b and c) of MnO₂-80°C-1, MnO₂-80°C-2.

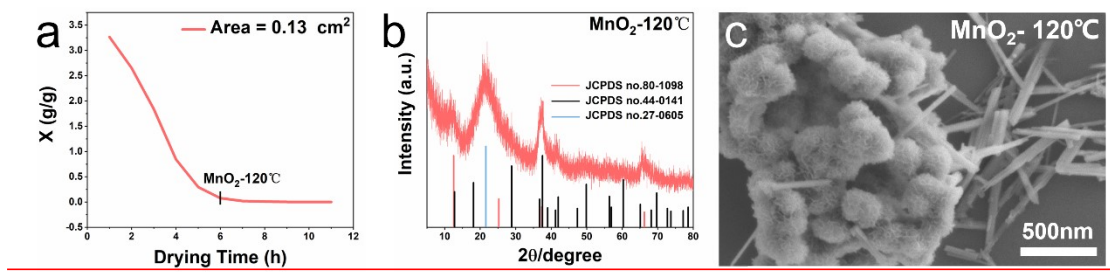


Fig. S6 The drying rate curves (a) in the case of Area = 0.13 cm², XRD patterns (b) and SEM images (c) of MnO₂-120°C.

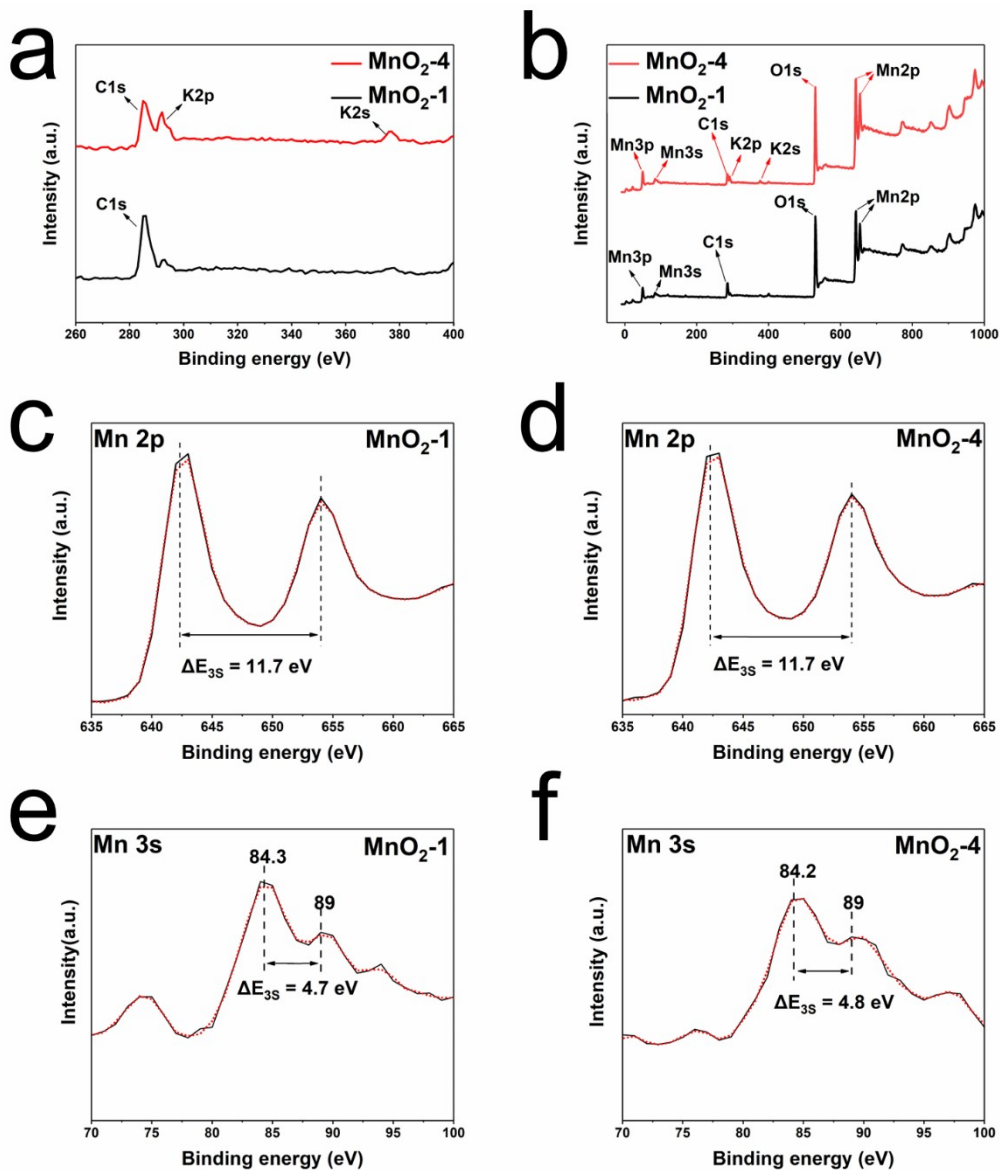


Fig. S7 (a) XPS spectra of C 1s, K 2p and K 2s for MnO₂-1 (δ -MnO₂) and MnO₂-4 (α -MnO₂). XPS survey spectra of MnO₂-1 (δ -MnO₂) and MnO₂-4 (α -MnO₂) (b). Mn 2p XPS spectra of the MnO₂-1 (c) and MnO₂-4 (d). Mn 3s XPS spectra of the MnO₂-1 (e) and MnO₂-4 (f).



$\delta\text{-MnO}_2$



$\alpha\text{-MnO}_2$

Fig. S8 Picture of synthesized MnO₂-1 ($\delta\text{-MnO}_2$) (left) and MnO₂-4 ($\alpha\text{-MnO}_2$) (right).

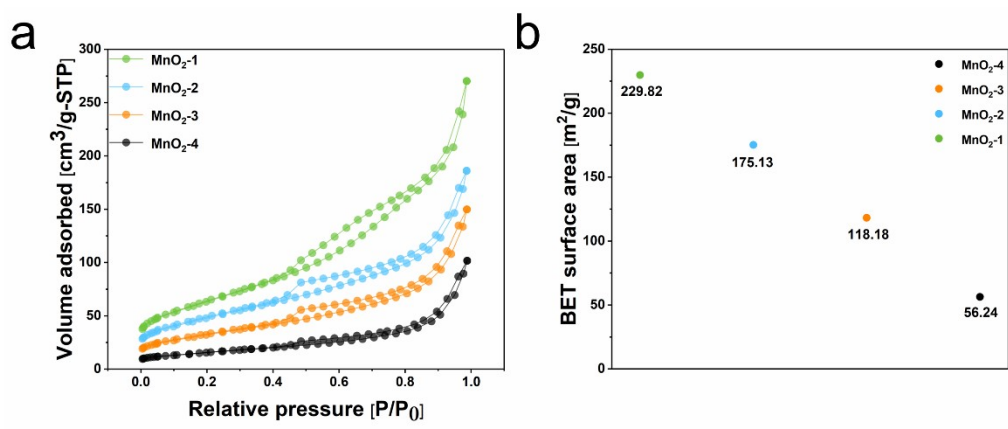


Fig. S9 Brunauer-Emmett-Teller (BET) analysis of MnO₂-1, MnO₂-2, MnO₂-3, and MnO₂-4.

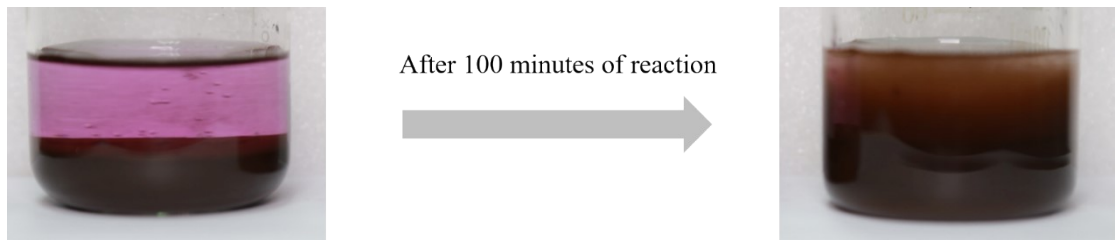


Fig. S10 Photo of solution after 100 minutes of thermal reaction.

Table S1 Comparison of specific capacitance between MnO₂ based materials

Electrode	Current density (A g ⁻¹)	Specific capacitance (F g ⁻¹)	Electrolyte	Ref.
δ-MnO ₂ +α-MnO ₂	1.8	178	LiCl	1
Co ₉ S ₈ @ MnO ₂	1	711.5	NaSO4	2
δ-MnO ₂ @α-MnO ₂	0.25	206	Na ₂ SO ₄	3
MnO _x @rGO	1	405	KOH	4
Fe: MnO ₂	2	173	Na ₂ SO ₄	5
K _{0.17} MnO ₂	1	206	K ₂ SO ₄	6
α-MnO ₂	0.5	535	KOH	7
MnO ₂	3	304	Na ₂ SO ₄	8
MnO ₂ -TEA	1	417.5	Na ₂ SO ₄	9
δ-MnO ₂	1	565	KOH	This work

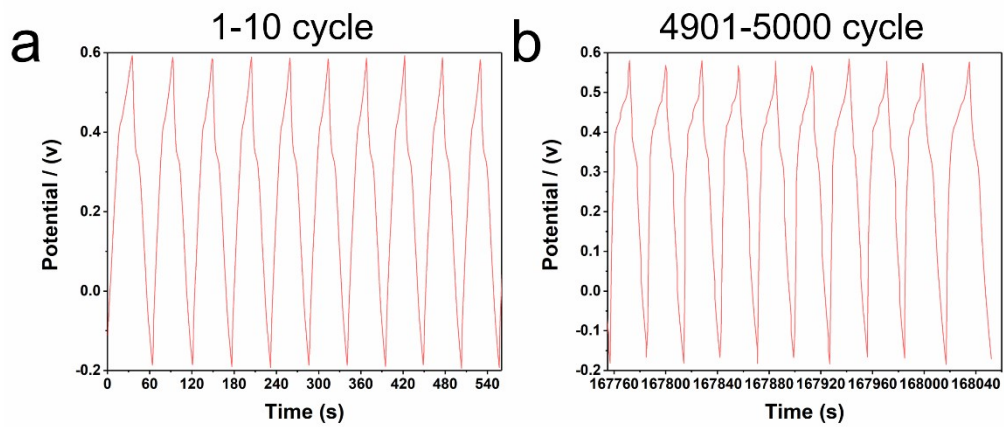


Fig. S11 The cycling tests of $\text{K}^+/\delta\text{-MnO}_2$ electrode at the 10 A g^{-1} .

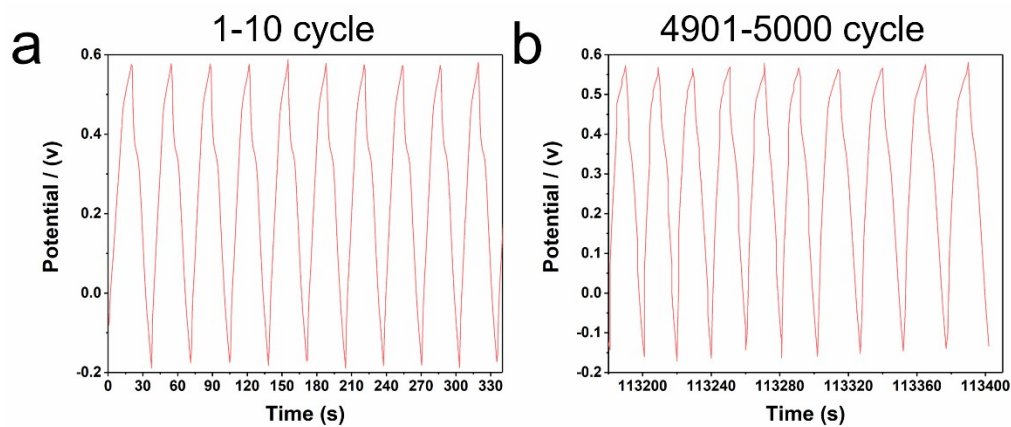


Fig. S12 The cycling tests of α -MnO₂ electrode at the 10 A g⁻¹.

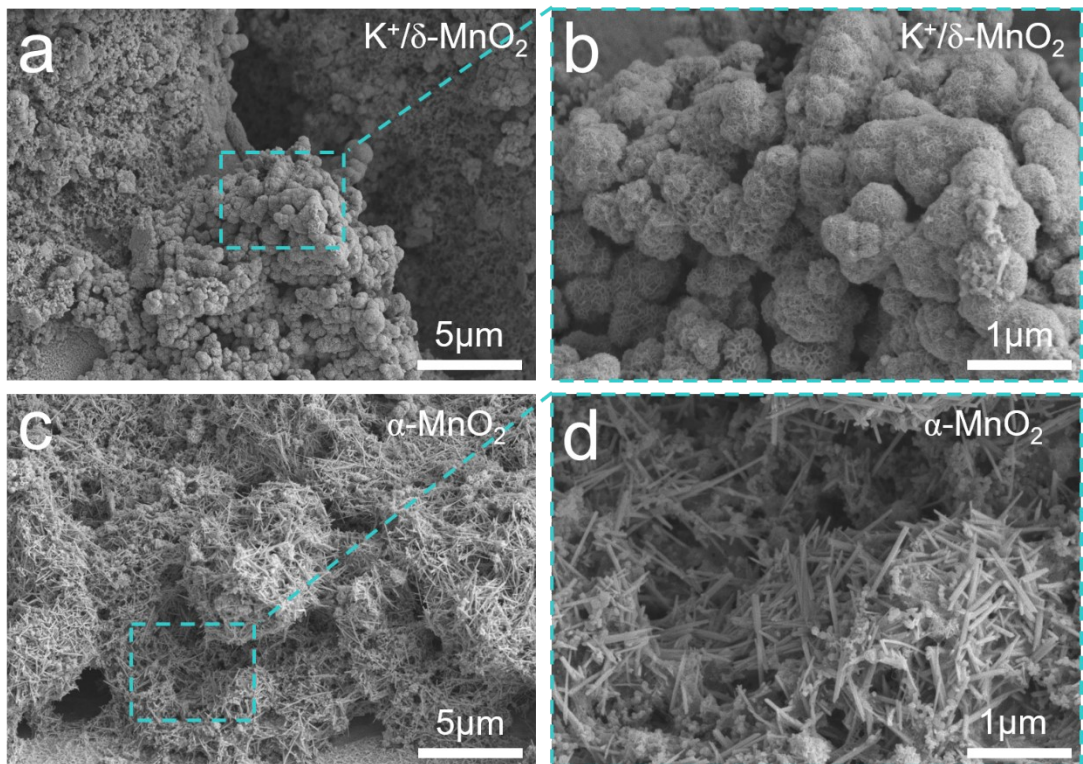


Fig. S13 SEM images of the (a, b) $\text{K}^+/\delta\text{-MnO}_2$ electrode and (c, d) $\alpha\text{-MnO}_2$ electrode after 5000 cycles at 10 A g^{-1} .

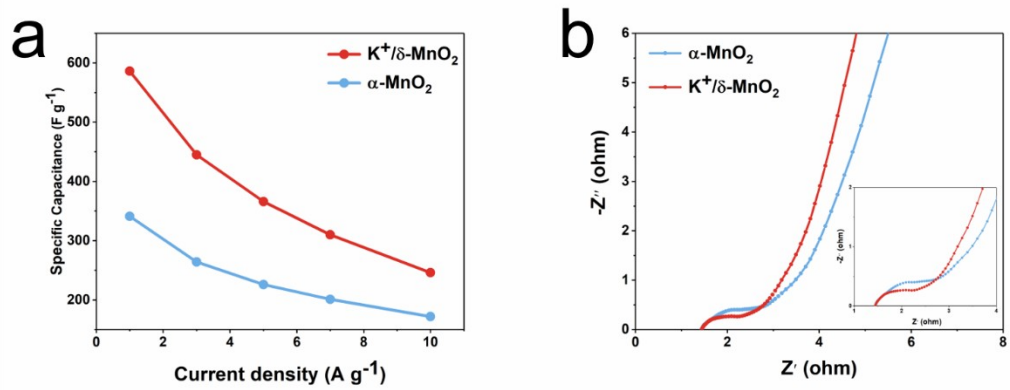


Fig. S14 (a) specific capacitance of $\text{K}^+/\delta\text{-MnO}_2$ and $\alpha\text{-MnO}_2$ at a series of current densities; (b) EIS curves of $\text{K}^+/\delta\text{-MnO}_2$ and $\alpha\text{-MnO}_2$.

References

- 1 C. R. Zhu, L. Yang, J. K. Seo, X. Zhang, S. Wang, J. Shin, D. L. Chao, H. Zhang, Y. S. Meng and H. J. Fan, *Materials Horizons*, 2017, **4**, 415-422.
- 2 Q. Li, M. Liu, F. Huang, X. Zuo, X. Wei, S. Li and H. Zhang, *Chemical Engineering Journal*, 2022, **437**, 135494.
- 3 T. Hatakeyama, N. L. Okamoto and T. Ichitsubo, *Journal of Solid State Chemistry*, 2022, **305**, 122683.
- 4 F. Jing, Z. Ma, J. Wang, Y. Fan, X. Qin and G. Shao, *Chemical Engineering Journal*, 2022, **435**, 135103.
- 5 D. P. Dubal, W. B. Kim and C. D. Lokhande, *Journal of Physics and Chemistry of Solids*, 2012, **73**, 18-24.
- 6 J. B. Zhu, Q. Y. Li, W. T. Bi, L. F. Bai, X. D. Zhang, J. F. Zhou and Y. Xie, *Journal of Materials Chemistry A*, 2013, **1**, 8154-8159.
- 7 B. S. Yin, S. W. Zhang, H. Jiang, F. Y. Qu and X. Wu, *Journal of Materials Chemistry A*, 2015, **3**, 5722-5729.
- 8 Z.-H. Huang, Y. Song, D.-Y. Feng, Z. Sun, X. Sun and X.-X. Liu, *ACS Nano*, 2018, **12**, 3557-3567.
- 9 A. Q. Zhang, R. Zhao, L. Y. Hu, R. Yang, S. Y. Yao, S. Y. Wang, Z. Y. Yang and Y. M. Yan, *Advanced Energy Materials*, 2021, **11**.